

Featuring work from the group of Prof. Hong-Bo Sun at the college of Electronic Science and Engineering, Jilin University, Changchun, China.

Title: Localized flexible integration of high-efficiency surface enhanced Raman scattering (SERS) monitors into microfluidic channels

Hierarchical silver micronanostructures, fabricated by femtosecond laser direct writing induced photoreduction, can be integrated freely inside a microchannel as high efficiency SERS monitors for on-chip detection.

As featured in:



See Hong-Bo Sun *et al.*,
Lab Chip, 2011, **11**, 3347.

RSC Publishing

www.rsc.org/loc

Registered Charity Number 207890

Cite this: *Lab Chip*, 2011, **11**, 3347

www.rsc.org/loc

TECHNICAL NOTE

Localized flexible integration of high-efficiency surface enhanced Raman scattering (SERS) monitors into microfluidic channels†

Bin-Bin Xu,^a Zhuo-Chen Ma,^a Lei Wang,^a Ran Zhang,^a Li-Gang Niu,^a Zhe Yang,^b Yong-Lai Zhang,^a Wan-Hua Zheng,^c Bing Zhao,^b Ying Xu,^a Qi-Dai Chen,^a Hong Xia^{*a} and Hong-Bo Sun^{*ad}

Received 10th May 2011, Accepted 28th July 2011

DOI: 10.1039/c1lc20397e

We report here a facile approach for flexible integration of high efficiency surface enhanced Raman scattering (SERS) monitors in a continuous microfluidic channel. In our work, femtosecond laser direct writing was adopted for highly localizable and controllable fabrication of the SERS monitor through a multi-photon absorption (MPA) induced photoreduction of silver salt solution. The silver substrate could be shaped into designed patterns, and could be precisely located at the desired position of the microchannel bed, giving the feasibility for real-time detection during reactions. SEM and TEM images show that the silver substrates were composed of crystallized silver nanoplates with an average thickness of 50 nm. AFM results reveal that the substrates were about 600 nm in height and the surface was very rough. As representative tests for SERS detection, *p*-aminothiophenol (*p*-ATP) and flavin adenine dinucleotide (FAD) were chosen as probing molecules for microfluidic analysis at visible light (514.5 nm) excitation, exhibiting an enhancement factor of $\sim 10^8$. In addition, the combination of the SERS substrate with the microfluidic channel allows detection of inactive analytes through *in situ* microfluidic reactions.

Introduction

In recent years, brilliant progress in lab-on-a-chip (LoC) systems has unfolded in virtue of its numerous advantages such as low dosage, high safety, high efficiency and high sensitivity compared with conventional macroscopic systems. Especially, as high throughput analytical microdevices, LoC systems show great potential for high sensitivity detection of various chemical and biological molecules. To date, a variety of detecting methods have been successfully applied in microfluidic systems, for instance, laser induced fluorescence (LIF),¹ UV-visible absorption,² chemiluminescence,³ mass spectrometry (MS),⁴ inductively coupled plasma-atom emission spectroscopy (ICP-AES),⁵ thermal lens microscopy,⁶ and biosensor.⁷ Among these analytical methods, LIF has been widely used as a high sensitivity

optodetection technique. The reported detecting concentration was as low as $\sim 10^{-13}$ mol L⁻¹, in other words, reaching the 'single molecule detection' range. However, the fluorescence detection methods have been restrained when applied to analytes or products that have no fluorescence. Therefore, fluorescent molecule tagging⁸ beforehand is essential for detection. In addition, the fluorescence detection cannot provide sufficient structural information of analytes, which significantly limited their further applications in LoC.

Raman spectra provide unique molecular fingerprints composed of many narrow-band peaks corresponding to sub-molecular vibrational modes in each functional group, making it possible to identify the species of the molecules even facing multiple analytes. However, Raman scattering suffers from low scattering cross-sections which result in very low sensitivity. The problem is solved by the surface enhanced Raman scattering (SERS) technique, whereby molecular Raman scattering cross-sections could be significantly amplified due to the adsorption of analytes on SERS substrates (*e.g.* rough noble metals or transition metal surfaces). As a result, SERS has become a powerful method for probing the structural properties of various analytes. Typical enhancement factors of SERS substrates are in the range of 10^6 to 10^9 , in some special cases, also reaching 'single molecule level' detection.⁹⁻¹² Undoubtedly, SERS would be a significant supplementary detection technology for LoC systems.¹³⁻²¹

Combined with SERS substrates, the Raman spectra detection of analytes in a microfluidic channel could be accomplished in

^aState Key Laboratory on Integrated Optoelectronics, College of Electronic Science and Engineering, Jilin University, 2699 Qianjin Street, Changchun, 130012, China. E-mail: hxia@jlu.edu.cn; hbsun@jlu.edu.cn; Fax: +86 431 85168281; Tel: +86 431 85168281

^bState Key Laboratory of Supramolecular Structure and Materials, Jilin University, Qianjin Street 2699, Changchun, 130012, P.R. China

^cInstitute of Semiconductors, Chinese Academy of Sciences, Beijing P.O. Box 912, Beijing, 100083, P.R. China

^dCollege of Physics, Jilin University, 2699 Qianjin Street, Changchun, 130012, China

† Electronic supplementary information (ESI) available: Absorption of silver ions, SEM of nanoplates in low and high laser power, the Raman spectrum of the solid *p*-ATP and the SERS spectrum of adsorbed *p*-ATP molecules. See DOI: 10.1039/c1lc20397e

a much more efficient manner. For instance, Lee *et al.*^{13–15} reported a robust fabrication of silver nanowell SERS substrates by soft lithography, which promises label free detection of biochemical reactions in multiplexed aqueous environments. Choo *et al.*^{16,17} used silver colloids as reproducible SERS substrates for detection of DNA, cyanide water pollutant, and hazardous materials in an alligator teeth-shaped microfluidic channel. Strehle *et al.* gave the example of SERS detection in segmented flow devices by using gold colloids as reproducible SERS substrates.¹⁸ Despite the fact that SERS substrates are successfully adopted by LoC systems, there are still a lot of problems in compatibility, efficiency and controllability in real microfluidic analysis. For example, the colloidal SERS substrates might bring significant disturbance to the subsequent reaction and analysis when used in a continuous microflow. Therefore, it is still a challenge to flexibly integrate SERS substrates into the microfluidic channel in a controlled fashion.

Previously, we have proved femtosecond laser fabrication a powerful nanotechnology for *in situ* functionalization of LoC systems.^{22–27} In this letter, we present a flexible integration of the silver SERS monitor in a ready microfluidic channel for high efficiency target molecule detection. Here, femtosecond laser induced photoreduction of silver ions was used for direct fabrication of silver SERS substrates.²⁴ Novel silver substrates with designable sizes and shapes could be precisely located at any position of the microchannel, indicating the flexibility of this method. As representative tests, *p*-aminothiophenol (*p*-ATP) and flavin adenine dinucleotide (FAD) were used for microfluidic analysis, the signal enhancement of 8 orders of magnitude could be achieved in the silver substrate. The integrated SERS substrate in the microfluidic channel exhibits capability for detection of inactive analytes through designed reactions.

Experimental

Preparation of the silver precursor

In a typical synthesis of the transparent silver-gilt solution, 0.08 M silver nitrate (AgNO_3) aqueous solution and 0.06 M trisodium citrate ($\text{C}_6\text{H}_5\text{O}_6\text{Na}_3$) were mixed under stirring at room temperature. Then a proper amount of aqueous ammonia was dripped into the mixture until a clear solution was obtained.

Preparation of the microfluidic chip

The microchannel was fabricated on a normal glass substrate using the combination of photolithography and wet-etching techniques. Before usage, the chip was cleaned ultrasonically by acetone and alcohol for ten minutes, respectively. Then it was further rinsed by distilled water and dried with nitrogen gas.

Femtosecond laser fabrication of SERS substrates in the microchannel

For fabrication of the silver SERS substrate in the microchannel, a femtosecond laser pulse (central wavelength: 800 nm; pulse width: 120 fs; and repetition rate: 80 MHz) was tightly focused into the silver precursor by a 100 \times oil immersion objective lens with a high numerical aperture ($\text{NA} = 1.40$). The focal spot was scanned laterally by steering a two-galvano-mirror set and

keeping along the optical axis by a piezo stage, both with high motion accuracy.^{28,29} The silver nanoplate was induced under the conditions of 10 mW laser power before the objective lens and of 1000 μs exposure duration at each dot. All the processes of fabrication were controlled by a computer exactly. The patterned silver nanoplates were rinsed in distilled water for 10 min to remove the residual silver-ion solution.

Characterization

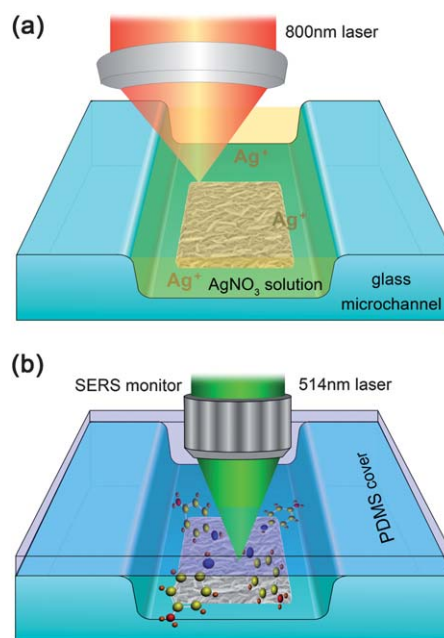
The extinction spectra were measured on a Shimadzu UV-3600 spectrometer. The surface morphologies of the samples were measured on a JEOL JSM-6700F field emission scanning electron microscope (FE-SEM) operating at 3.0 keV.

The crystalline structures of the samples were characterized through a JEOL-2100F high-resolution transmission electron microscope (HRTEM) functioning at 200 kV. Surface-enhanced Raman spectra were measured on a JOBIN YVON T64000 equipped with a liquid-nitrogen-cooled argon ion laser at 514.5 nm (Spectra-Physics Stabilite 1017) as excitation source (the laser power used was about 40 μW at the samples with an average spot size of 1 μm in diameter). The spectral resolution was 4 cm^{-1} at the excitation wavelength.

Results and discussion

Integration of silver SERS substrates inside microchannels

Scheme 1 shows the fundamental concept of our flexible integration of the silver SERS substrate inside a microchannel and its application illustration as a SERS monitor for target molecule detection. Firstly, a femtosecond laser pulse was tightly focused on the microchannel bed to fabricate the SERS substrates



Scheme 1 Sketch of femtosecond laser fabrication of the silver SERS substrate inside a microfluidic channel (a), and the application of this SERS monitor for target molecule detection at visible light (514.5 nm) excitation (b).

through photoreduction of the silver precursor. The absorption spectrum of the silver precursor shows only one absorption band at ~ 300 nm (ESI†, Fig. S1), so the inherent mechanism might be a multiphoton absorption (MPA) induced photoreduction.²⁴ After fabrication, the microchannel with the silver SERS substrate was sealed with a polydimethylsiloxane (PDMS) film for analysis (Scheme 1b).

Taking advantage of the designability of laser processing, our photoreduced silver substrate could be created at any desired position and with arbitrary shapes. In other words, the SERS substrate could be fabricated according to the chip size and geometry, indicating the flexibility of this integration. As shown in Fig. 1, by precise control of the laser processing system through a computer, silver substrate arrays with different shapes and sizes were patterned in the microchannel bed (75 μm wide and 20 μm deep). Fig. 1a shows a 4×4 array of 5.5 μm silver square. Fig. 1b exhibits a 3×3 array of 11.0 μm square. Beside square arrays, the silver substrate could also be shaped into uniform circle arrays (Fig. 1c). In Fig. 1d, round silver substrates were fabricated at the branch of a “Y” shaped microchannel. When two reactants pass the Y channel and mix together, these combined SERS substrates might monitor both the reactants and the products of the reaction, giving the feasibility for real-time detection. It is worth pointing out that this designable fabrication of the SERS substrate is of benefit to the improvement of both compatibility and efficiency, therefore, showing promising potential for chip use. Additionally, the fabrication of such silver substrates is not limited to glass chips, general PDMS chips could also be used for this post-integration.

Characterization of silver SERS substrates

The surface morphology of the silver SERS substrate was characterized by SEM. As shown in Fig. 2a and b, the substrate is composed of vertical silver nanoplates, which would enlarge the effective surface area and increase the probability for capturing

analyte molecules. The magnified image gives a much clearer observation of the nanoplates (Fig. 2b). It could be clearly identified that there are a lot of nanoparticles on the surface of the nanoplates which contribute to an improved roughness and give rise to SERS enhancement. In our experiment, the laser power plays a very important role on the formation of nanoplates, fabrication under too low or too high laser power will result in the formation of irregular morphology (ESI†, Fig. S2). The statistical result reveals that the average amount density of the silver nanoplates is about $3 \times 10^6 \text{ mm}^{-2}$, and the thickness of the silver nanoplates is in the range of 20 nm to 80 nm (mostly 50–60 nm, Fig. 2c).

In order to investigate the crystalline structure of these silver nanoplates, the sample was also characterized by high-resolution transmission electron microscopy (HRTEM). As shown in Fig. 2d, the silver nanoplates are crystalline, the lattice of the (111) and (200) planes could be clearly identified from the image, confirming their polycrystalline properties. The interplanar spacings of these two planes are 0.24 and 0.20 nm respectively, which are very close to the theoretical values (0.236 and 0.201 nm). The inset of Fig. 2d is the electron diffraction pattern of this silver nanoplate, the bright rings correspond to the (111), (200), (220) and (311) silver planes respectively, confirming its polycrystalline structure.

As an integrated functional segment, the compatibility of the SERS substrate was very important for the whole LoC system. In this work, the surface of our silver SERS substrate was characterized with Atomic Force Microscopy (AFM). As shown in Fig. 3a, a large number of vertical nanoplates could be identified from the image. The unique vertical nanoplates make the surface very rough, which is of benefit to the SERS detection. Fig. 3b shows a 3D view of this surface. The height of our silver substrate is considered as a key factor of its compatibility, because the high

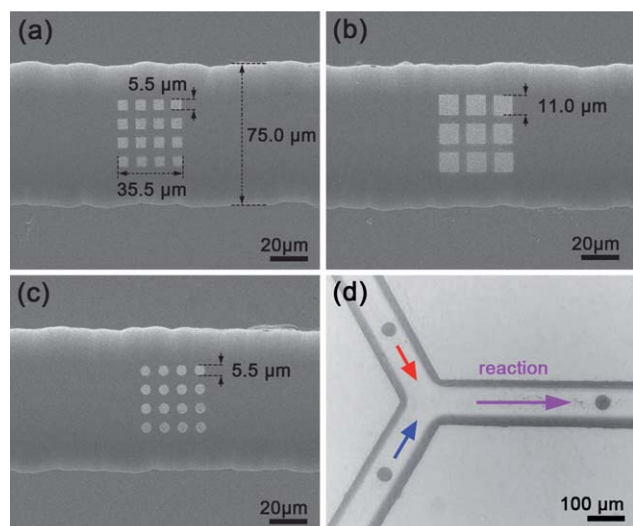


Fig. 1 SEM images of silver SERS substrates integrated in the microfluidic channel with different patterns and sizes. (a) 4×4 5.5 μm square arrays; (b) 3×3 11.0 μm square arrays; (c) 4×4 circle arrays with a diameter of 5.5 μm ; and (d) silver SERS substrates at different positions of the microchannel.

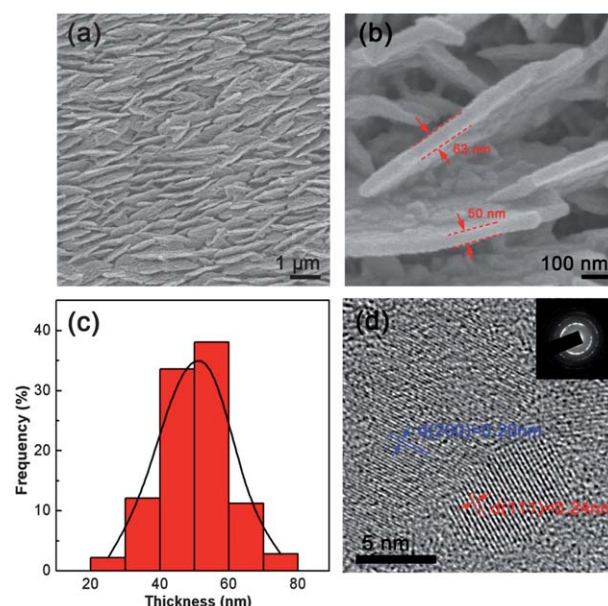


Fig. 2 (a) SEM image of the silver SERS substrate; (b) magnified SEM image of the silver nanoplates on the substrate; (c) the thickness distribution of the silver nanoplates which is calculated based on 200 nanoplates; and (d) HR-TEM image of one silver nanoplate, the inset is the diffraction pattern.

surface would result in intrusions of the microfluid. The height profile of the white line in Fig. 3c shows that our silver SERS substrate is about 600 nm in height (Fig. 3d), which is small enough for chip use considering the depth of the microchannel which is about 30 μm .

SERS detection

After the silver SERS substrate fabrication, the microfluid of *p*-aminothiophenol (*p*-ATP, 10^{-9} M, for structural information see ESI†) solutions was used for detection in the microchannel. As an important probe molecule in SERS detection, *p*-ATP is widely used because the thiol group could react with metal surfaces. Fig. 4a shows the Raman spectra of *p*-ATP measured at different positions of the silver SERS substrate, five typical bands at 1573, 1439, 1391, 1142, and 1075 cm^{-1} could be observed in the spectrum which are consistent with its solid Raman spectrum (ESI†, Fig. S3). The predominant peaks located at 1595 and 1089 cm^{-1} (ESI†, Fig. S3) shift to 1573 and 1075 cm^{-1} , respectively, which are assigned to the a_1 modes of the *p*-ATP molecules. Notably, the bands at 1142, 1391, 1433, and 1574 cm^{-1} which are assigned to the b_2 modes of the *p*-ATP were selectively enhanced according to the charge transfer (CT) mechanism.^{30–32} The simultaneous enhancement of a_1 modes and b_2 modes indicates that both the electromagnetic (EM) and CT mechanisms contribute in the enhancement. The presence of the broad peak at ~ 213 cm^{-1} is assigned to the Ag-SH stretching.

To evaluate the enhancement ability of our silver substrate, the enhancement factor (EF) was calculated according to the following formula:

$$EF = (I_{\text{SERS}}/N_{\text{ads}})/(I_{\text{bulk}}/N_{\text{bulk}})$$

where I_{SERS} and I_{bulk} are the intensities of a vibration mode in the SERS spectrum and in the normal Raman spectrum, respectively. N_{ads} and N_{bulk} are the number of molecules probed in the SERS spectrum and in the normal Raman spectrum, respectively. In our result, the EF value was calculated to be

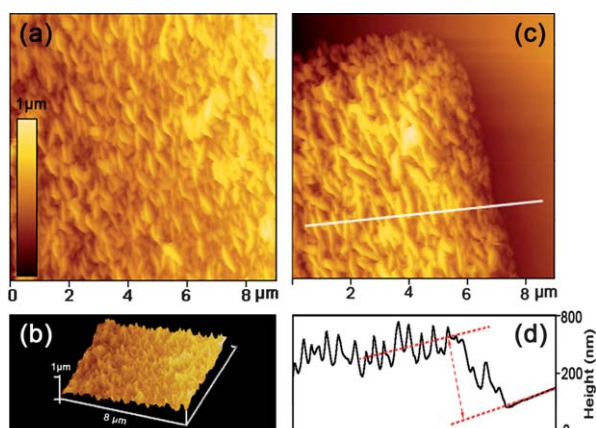


Fig. 3 AFM characterization of the silver SERS substrate. (a) The surface of one silver substrate; (b) 3D view of the silver substrate; (c) one corner of the silver substrate and (d) the height profile along the white line.

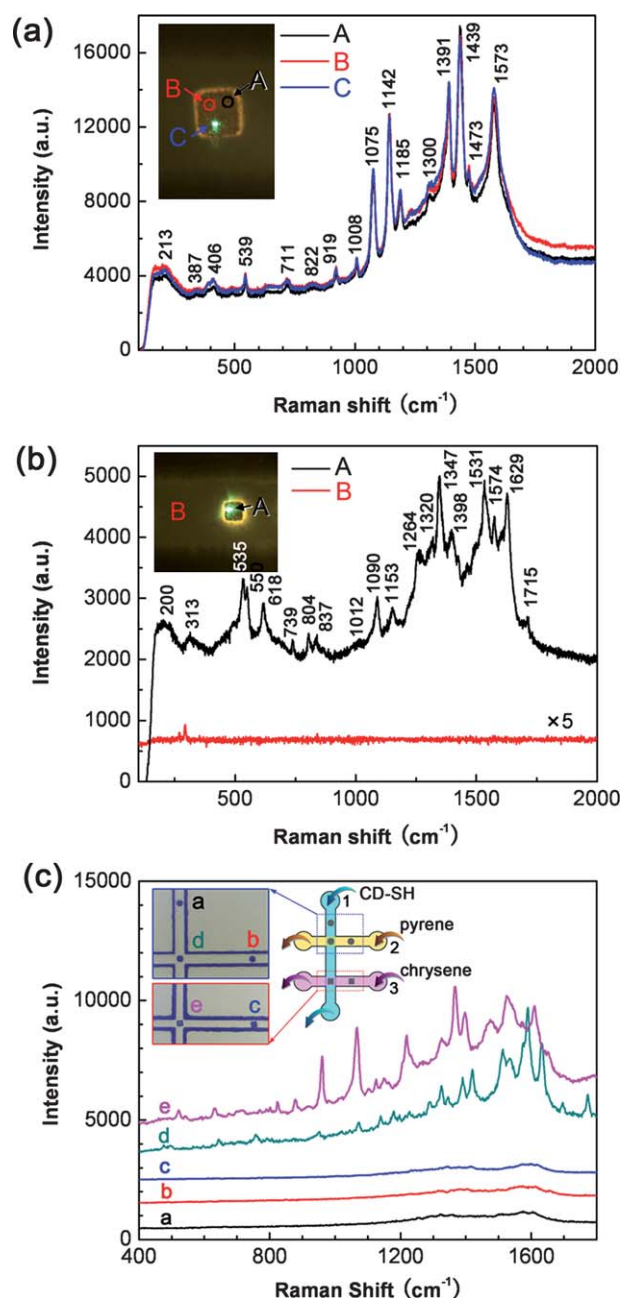


Fig. 4 (a) Raman spectra of *p*-aminothiophenol (*p*-ATP) measured at different positions of the silver SERS substrate, the inset is an optical microscopic image of the silver SERS substrate and different measure positions; (b) Raman spectra of flavin adenine dinucleotide (FAD) measured on and beside the silver SERS substrate, the inset is an optical microscopic image of the silver SERS substrate and the measure position. (c) Raman spectra measured on silver SERS substrates at different positions of the microchannel (a–e). The inset is the scheme of the experiments and an optical microscopy image of the microchannel with silver SERS substrates.

4×10^8 , and the detection limit was as low as 10^{-10} M (for calculation details see the ESI†, Fig. S4 and S5). The concentration–intensity linear relationship is also shown in Fig. S5†. In the test of *p*-ATP, as shown in Fig. 4a, we chose three locations (A, B and C) to detect the SERS signals, and the peak intensity

error was less than 3%, indicating the excellent uniformity of our SERS substrate.

In our experiment, flavin adenine dinucleotide (FAD, 10^{-6} M), a redox cofactor involved in several important reactions in metabolism, was also chosen as a representative candidate for biomolecule detection. Typical peaks of FAD located at 535, 1090, 1347, 1531, 1574 and 1629 cm^{-1} (ref. 33 and 34) could be easily identified from the spectrum measured on the active silver substrate. As a comparison, the SERS signals beside the substrate (position B, the inset of Fig. 4b) were negligible even after being amplified by 5 times, confirming the efficacy of our silver substrates.

To demonstrate the merits of our flexible integrated SERS monitor, five SERS substrates were fabricated in a crossed microchannel system. As shown in Fig. 4c, per-6-deoxy-(6-thio)- β -cyclodextrin (CD-SH) was firstly injected into channel 1 with the help of a pump, whereas channels 2 and 3 were sealed up to avoid contamination. So substrates a, d and e were modified with CD-SH due to the interaction between the silver and the mercapto group. Then polycyclic aromatic hydrocarbon (PAH) molecules such as pyrene and chrysene were injected into channels 2 and 3, respectively. As reported elsewhere, PAH molecules (substrates b and c) have negligible SERS signals due to the low affinity to the metallic surface.³⁵ However, in the crossed region, SERS signals of pyrene and chrysene could be easily detected due to the formation of complex with CD-SH.³⁵ These results show that our locally integrated SERS substrates allow real-time detection of analytes during chemical reactions, thus giving the feasibility for *in situ* detection at different positions.

Conclusions

In conclusion, we have fabricated a patterned silver substrate at the bottom of a microchannel by femtosecond laser induced photoreduction. The silver substrate was designed as a noninvasive and high-efficiency surface enhanced Raman scattering (SERS) monitor for LoC systems. As the laser processing has its unique merit of designability, this *in situ* fabrication of SERS substrates could be shaped into various patterns and located at any position of the microchannel. In the SERS detection, *p*-aminothiophenol (*p*-ATP) and flavin adenine dinucleotide (FAD) were used for microfluidic analysis, exhibiting an electromagnetic enhancement factor of $\sim 10^8$. This flexible integration of the silver SERS substrate would promote the use of the Raman spectral analysis in LoC systems.

Acknowledgements

The authors acknowledge the financial support from 973 Program under grant #2011CB013005 and from NSFC under grant #60978048 and 90923037.

References

- 1 R. F. Renzi, J. Stamps, B. A. Horn, S. Ferko, V. A. VanderNoot, J. A. West, R. Crocker, B. Wiedenman, D. Yee and J. A. Fruetel, *Anal. Chem.*, 2005, **77**, 435–441.
- 2 H. Nakanish, T. Nishimoto, A. Arai, H. Abe, M. Kanai, Y. Fujiyama and T. Yoshida, *Electrophoresis*, 2001, **22**, 230–234.
- 3 X. Huang and J. Ren, *Electrophoresis*, 2005, **26**, 3595–3601.
- 4 L. Jiang, Y. Lu, Z. Dai, M. Xie and B. Lin, *Lab Chip*, 2005, **5**, 930–934.
- 5 Q. Xue, F. Foret, Y. M. Dunayevskiy, P. M. Zavracky, N. E. McGruer and B. L. Karger, *Anal. Chem.*, 1997, **69**, 426–430.
- 6 A. Y. Hui, G. Wang, B. Lin and W. T. Chan, *J. Anal. At. Spectrom.*, 2006, **21**, 134–140.
- 7 T. Kitamori, M. Tokeshi, A. Hibara and K. Sato, *Anal. Chem.*, 2004, **76**, 52A–60A.
- 8 U. Kim and H. T. Soh, *Lab Chip*, 2009, **9**, 2313–2318.
- 9 K. Kneipp, H. Kneipp and J. Kneipp, *Acc. Chem. Res.*, 2006, **39**, 443–450.
- 10 M. Moskovits, *J. Raman Spectrosc.*, 2005, **36**, 485–496.
- 11 X. M. Qian and S. M. Nie, *Chem. Soc. Rev.*, 2008, **37**, 912–920.
- 12 L. Chen and J. Choo, *Electrophoresis*, 2008, **29**, 1815–1828.
- 13 H. Cho, B. Lee, G. L. Liu, A. Agarwal and L. P. Lee, *Lab Chip*, 2009, **9**, 3360–3363.
- 14 A. Y. Lau, L. P. Lee and J. W. Chan, *Lab Chip*, 2008, **8**, 1116–1120.
- 15 D. Choi, T. Kang, H. Cho, Y. Choi and L. P. Lee, *Lab Chip*, 2009, **9**, 239–243.
- 16 L. X. Quang, C. Lim, G. H. Seong, J. Choo, K. J. Dob and S. K. Yoob, *Lab Chip*, 2008, **8**, 2214–2219.
- 17 T. Park, S. Lee, G. H. Seong, J. Choo, E. K. Lee, Y. S. Kim, W. H. Ji, S. Y. Hwang, D. G. Gweon and S. Lee, *Lab Chip*, 2005, **5**, 437–442.
- 18 K. R. Strehle, D. Cialla, P. Rosch, T. Henkel, M. Kohler and J. Popp, *Anal. Chem.*, 2007, **79**, 1542–1547.
- 19 Y. Han, X. Lan, T. Wei, H. L. Tsai and H. Xiao, *Appl. Phys. A: Mater. Sci. Process.*, 2009, **97**, 721–724.
- 20 K. Sun, Z. Wang and X. Jiang, *Lab Chip*, 2008, **8**, 1536–1543.
- 21 I. Barbulovic-Nad, S. H. Au and A. R. Wheeler, *Lab Chip*, 2010, **10**, 1536–1542.
- 22 J. Wang, Y. He, H. Xia, L. G. Niu, R. Zhang, Q. D. Chen, Y. L. Zhang, Y. F. Li, S. J. Zeng, J. H. Qin, B. C. Lin and H. B. Sun, *Lab Chip*, 2010, **10**, 1993–1996.
- 23 Y. Tian, Y. L. Zhang, J. F. Ku, Y. He, B. B. Xu, Q. D. Chen, H. Xia and H. B. Sun, *Lab Chip*, 2010, **10**, 2902–2905.
- 24 B. B. Xu, H. Xia, L. G. Niu, Y. L. Zhang, K. Sun, Q. D. Chen, Y. Xu, Z. Q. Lv, Z. H. Li, H. Misawa and H. B. Sun, *Small*, 2010, **6**, 1762–1766.
- 25 T. W. Lim, Y. Son, Y. J. Jeong, D. Y. Yang, H. J. Kong, K. S. Lee and D. P. Kim, *Lab Chip*, 2011, **11**, 100–103.
- 26 Y. L. Zhang, Q. D. Chen, H. Xia and H. B. Sun, *Nano Today*, 2010, **5**, 435–448.
- 27 D. Wu, Q. D. Chen, L. G. Niu, J. N. Wang, J. Wang, R. Wang, H. Xia and H. B. Sun, *Lab Chip*, 2009, **9**, 2391–2394.
- 28 J. Wang, H. Xia, B. B. Xu, L. G. Niu, D. Wu, Q. D. Chen and H. B. Sun, *Opt. Lett.*, 2009, **34**, 581–583.
- 29 H. Xia, J. Wang, Y. Tian, Q. D. Chen, X. B. Du, Y. L. Zhang, Y. He and H. B. Sun, *Adv. Mater.*, 2010, **22**, 3204–3207.
- 30 M. Osawa, N. Matsuda, K. Yoshii and I. Uchida, *J. Phys. Chem.*, 1994, **98**, 12702–12707.
- 31 Z. Lu, W. Ruan, J. Yang, W. Xu, C. Zhao and B. Zhao, *J. Raman Spectrosc.*, 2009, **40**, 112–116.
- 32 J. Zheng, Y. Zhou, X. Li, Y. Ji, T. Lu and R. Gu, *Langmuir*, 2003, **19**, 632–636.
- 33 R. A. Copeland, S. P. A. Fodor and T. G. Spiro, *J. Am. Chem. Soc.*, 1984, **106**, 3872–3874.
- 34 R. E. Holt and T. M. Cotton, *J. Am. Chem. Soc.*, 1989, **111**, 2815–2821.
- 35 Y. F. Xie, X. Wang, X. X. Han, X. X. Xu, W. Ji, Z. H. Qi, J. Q. Liu, B. Zhao and Y. Ozaki, *Analyst*, 2010, **135**, 1389–1394.